Available online at www.sciencedirect.com
ScienceDirect
Chinese Journal of Natural Medicines 2022, **20**(9): 669-678
doi: 10.1016/S1875-5364(22)60201-2
Chinese Journal of Natural Medicines

•Special topic•

20(*S*)-ginsenoside Rh1 alleviates T2DM induced liver injury *via* the Akt/FOXO1 pathway

SU Wen-Ya[1], FAN Mei-Ling[2], LI Ying[1], HU Jun-Nan[1], CAI En-Bo[1], ZHU Hong-Yan[1], SONG Ming-Jie[1, 3*], LI Wei[1, 3*]

[1] *College of Chinese Medicinal Materials, Jilin Agricultural University, Changchun 130118, China;*
[2] *Maternity Diagnosis & Treatment Center, the Affiliated Hospital of Changchun University of Chinese Medicine, Changchun 130021, China;*
[3] *National & Local Joint Engineering Research Center for Ginseng Breeding and Development, Changchun 130118, China*

Available online 20 Sep., 2022

[ABSTRACT] Diabetes-associated liver injury becomes a dominant hepatopathy, leading to hepatic failure worldwide. The current study was designed to evaluate the ameliorative effects of ginsenoside Rh1 (G-Rh1) on liver injury induced by T2DM. A T2DM model was established using C57BL/6 mice through feeding with HFD followed by injection with streptozotocin at 100 mg·kg^{-1}. Then the mice were continuously administered with G-Rh1 (5 and 10 mg·kg^{-1}), to explore the protective effects of G-Rh1 against liver injury. Results showed that G-Rh1 exerted significant effects on maintaining the levels of FBG and insulin, and ameliorated the increased levels of TG, TC and LDL-C induced by T2DM. Moreover, apoptosis in liver tissue was relieved by G-Rh1, according to histological analysis. Particularly, in diabetic mice, it was observed that not only the increased secretion of G6Pase and PEPCK in the gluconeogenesis pathway, but also inflammatory factors including NF-κB and NLRP3 were suppressed by G-Rh1 treatment. Furthermore, the underlying mechanisms by which G-Rh1 exhibited ameliorative effects was associated with its capacity to inhibit the activation of the Akt/FoxO1 signaling pathway induced by T2DM. Taken together, our preliminary study demonstrated the potential mechnism of G-Rh1 in protecting the liver against T2DM-induced damage.

[KEY WORDS] G-Rh1; Liver injury; Gluconeogenesis; PEPCK; G6Pase; Akt/FOXO1; Inflammation
[CLC Number] R965 **[Document code]** A **[Article ID]** 2095-6975(2022)09-0669-10

Introduction

Type 2 diabetes mellitus (T2DM), known as adult-onset diabetes, is characterized by high levels of blood sugar, insulin resistance and lack of insulin, which usually develops after the age of 35 to 40, and accounts for more than 90% of patients with diabetes [1]. The complications of T2DM include cardiovascular diseases, diabetic retinopathy and nephropathy which may cause stroke, blindness, and renal failure, and constitute the major challenge in diabetes management [2]. The liver is the main site of gluconeogenesis, and indispensable for the maintenance of glucose homeostasis by regulating its uptake/release and storage [3-5]. However, hyperglycemia in diabetes may induce hepatocyte injury through initiating inflammation, resulting in the development of hepatic diseases [6].

Insulin is a naturally occurring hormone that helps the body regulate blood glucose levels. It can also stimulate the liver to store excessive glucose in the form of glycogen and lipid [7]. Actually, insulin facilitated the suppression of hepatic gluconeogenesis by activating protein kinase B (Akt), which in turn deactivated the key gluconeogenic transcription factor, Forkhead Box O1 (FOXO1) [8, 9]. Then, FOXO1 directly bound to the promoters of genes encoding key rate-controlling enzymes, such as glucose-6-phosphatase (G6Pase) and phosphoenolpyruvate carboxylase (PEPCK), in the process of gluconeogenesis to strengthen their transcription under the contition of T2DM [10]. Akt was also involved in the inhibition of FOXO through phosphorylation, resulting in the translocation of FOXO from the nucleus to the cytoplasm [11]. Furthermore, chronic inflammation is recognized as a major feature of T2DM and associated with enhanced regulation of inflammatory factors. Nuclear factor kappa B

[Received on] 18-Feb.-2022
[Research funding] This work was supported by Jilin Science & Technology Development Plan (No. 20200301037RQ).
[*Corresponding author] Tel/Fax: 86-431-84533304, E-mails: songmingjie2017@126.com (SONG Ming-Jie); liwei7727@126.com (LI Wei)
These authors have no conflict of interest to declare.

(NF-κB) is a protein transcriptional factor involved in the development of inflammation upon activation by external stimuli, and its elevated secretion may lead to hyperlipidemia and insulin resistance, resulting in hepatocytic pathogenesis [12, 13]. When activated, NF-κB bound to regulatory DNA sequences, and triggered the production of a range of inflammatory cytokines, such as TNF-α and IL-1β [14]. The nucleotide-binding-domain (NBD)-and leucine-rich repeat (LRR)-containing (NLR) family, pyrin-domain-containing 3 (NLRP3) inflammasome was considered another pivotal factor for inflammation. Yet, NF-κB was required for NLRP3 activation: a NF-κB-dependent priming signal responsible for the up-regulation of IL-1β and NLRP3 was followed by a second one which involved with triggering the assembly and activation of the NLRP3 inflammasome [15]. In addition, numerous studies have shown that the PI3K/Akt signaling pathway regulates cell proliferation, differentiation, apoptosis, and migration through inhibiting the expression of downstream target protein NF-κB [16, 17]. Previous studies showed that ginsenoside Rg1 inhibited glucagon-induced hepatic gluconeogenesis through Akt-FOXO1 interaction [18, 19].

Ginseng (*Panax ginseng* C. A. Meyer) is a well-known medicinal herb that has been used for the treatment of diabetes in China and recognized worldwide [20]. According to previous studies, protopanaxatriol saponins were effective in the prevetion and treatment of T2DM [21], expeically ginsenoside Rh1 (G-Rh1) (Fig. 1A), a major biologically active components converted from ginsenoside Re [22, 23]. To date, it is unclear, however, whether G-Rh1 can relieve liver injury induced by T2DM. Based on the current findings, we speculated that G-Rh1 is involved in the regulation of hepatic gluconeogenesis and lipid metabolism *via* the Akt/FOXO1 signaling pathway, so as to modulate the risks of hyperlipidemia and inflammation induced by T2DM. To verify this hypothesis, we investigated whether G-Rh1 can inhibite FOXO1 expression to suppress the expression of G6Pase and PEPCK, and inhibit the activation of NLRP3 induced by T2DM to modulate inflammation using a mouse model.

Materials and Methods

Reagents

G-Rh1 (purity > 98% by HPLC) was converted from Re and purified by semi-preparative HPLC in our laboratory. High fat diet (HFD) consisting of 20% carbohydrate, 45% fat and 35% protein, was purchased from Research Diets Inc. (No. D12492, 60% kcal) and used for inducing diabetes in mice. Streptozocin (STZ) was purchased from Sigma (St. Louis, MO, USA). The alanine aminotransferase (ALT), aspartate aminotransferase (AST), triglyceride (TG), total cholesterol (TC), low-density lipoprotein cholesterol (LDL-C), high-density lipoprotein cholesterol (HDL-C) and hematoxylin-eosin (H&E) kits were obtained from Nanjing Jiancheng Bioengineering Research Institute (Nanjing, China). The insulin (INS) ELISA kit was purchased from R&D systems (Minneapolis, MN, USA). The rabbit anti-mouse monoclonal antibodies FOXO1, p-FOXO1, Akt and p-Akt, NF-κB and p-NF-κB, NLRP3, ASC, TNF-α, IL-1β, Caspase 1 and Cleaved Caspase 1 were purchased from Cell Signaling Technology (Danvers, MA, USA). The rabbit anti-mouse monoclonal antibodies G6Pase and PEPCK were purchased from Proteintech (Rosemont, IL, USA).

Animals and experimental design

A total of 40 male adult C57BL/6 mice, weighing 20−25 g, were purchased from Beijing Huafukang Experimental Animal Co., Ltd. (Certificate No. SCXK (Jing) 2014-0004). The mice were maintained at 22 ± 2 °C, 60% ± 10% humidity with 12 h light/dark cycle and free access to commercial pellet diet and water. All the mice were initially acclimatized to the environment for one week before T2DM induction. Animal investigations were performed according to the Regulations of Experimental Animal Administration issued by the Ethical Committee for Laboratory Animals at Jilin Agricultural University.

The mice were randomly divided into four groups: a normal group, a T2DM model group, and a T2DM + G-Rh1-L group and a T2DM + G-Rh1-H group. Briefly, mice in the normal group were injected with a certain volume of 0.5%

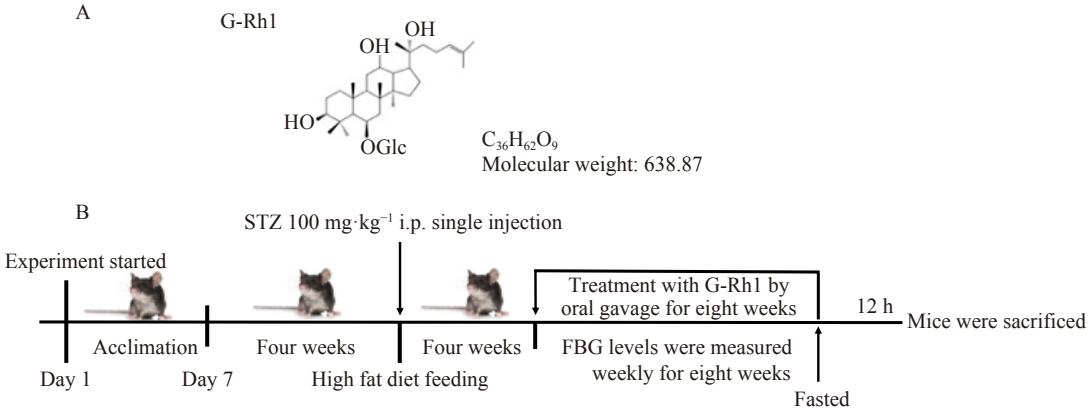

Fig. 1 Structure of G-Rh1 (A), and schematic representation for the induction of T2DM in C57BL/6 mice (B)

CMC-Na depending on body weight and received a standard balanced diet [24]. To induce T2DM, mice were fed with HFD for consecutive four weeks, followed by intra-peritoneal injection of streptozotocin (STZ) at 100 mg·kg^{-1} dissolved in a freshly prepared 0.1 mol·L^{-1} citrate buffer at pH 4.2−4.4. HFD feeding was conducted throughout the experiments [24]. To evaluate the effect of G-Rh1 on diabetes, four weeks after STZ injection, diabetic rats were administered by gastric gavage with G-Rh1 (5 and 10 mg·kg^{-1}) for eight weeks, and then divided into two groups, namely a T2DM + G-Rh1-L group and a T2DM + G-Rh1-H group, respectively. During G-Rh1 administration, the levels of fasting blood glucose (FBG) were measured weekly to determine the occurrence of hyperglycemia using an ACCU-CHEK Performa blood glucose monitoring system (Roche Diagnostics GmbH, Germany). Mice with blood glucose levels between 7.8 and 16.67 mmol·L^{-1} were considered to have hyperglycemia [5]. The mice were sacrificed after eight weeks of G-Rh1 treatment (Fig.1).

Detection of serum levels of ALT, AST and INS

The primary indicators for liver functions, alanine aminotransferase (ALT) and aspartate aminotransferase (AST), were measured using alanine and aspartate aminotransferase assay kits, respectively [25]. Briefly, after the mice were sacrificed, blood was collected before centrifugation at 1000 × *g* at 4 °C for 10 min. Then, the serum was taken, and incubated with specific substrates provided by the kits in a fresh 96-well plate at 37 °C for 30 min, followed by color development with specific color developers. The plates were read at a wavelength of 510 nm. The serum level of insulin (INS) was determined by an ELISA kit (R&D systems, USA) according to the manufacturer's instructions, and the absorbance was determined at 450 nm (Bio-Rad, Hercules, CA, USA).

Measurement of TC, TG, HDL-C, and LDL-C in serum

Blood samples of the mice were collected followed by centrifugation at 1000 × *g* at 4 °C for 10 min. The serum levels of total cholesterol (TC), triglycerides (TG), high-density lipoprotein cholesterol and low-density lipoprotein cholesterol (HDL-C and LDL-C) were detected according to the instructions of the corresponding commercial kits.

Histopathological examination

To examine histopathological changes in the liver, fresh hepatic tissues were fixed in 10% neutral formalin and then embedded in paraffin. The paraffin-embedded tissue blocks were cut into 5 μm-thick sections. Then, histological analysis was carried out and the sections were stained with H&E dye as previously described [25]. Finally, the pathological changes of the liver tissues were observed under an optical microscope (Leica, DM750, Solms, Germany).

Immunofluorescence staining

Immunofluorescence staining was performed to measure the levels of target proteins [26]. Briefly, deparaffinized and rehydrated liver sections (5 μm) were treated with citrate buffer at 0.01 mol·L^{-1}, pH 6.0 for 20 min. After washed with PBS for three times, the sections were incubated with 1% BSA at room temperature for another 10 min to block non-specific binding, before exposure to the following primary antibodies: mouse anti-Bax and anti-Bcl-2 at a ratio of 1 : 200 respectively at 4 °C overnight. Then, the sections were incubated with SABC-DyLight 488 (BOSTER, Wuhan, China) at 37 °C for 12 h, and stained with 4,6-diamidino-2-phenylindole (DAPI). The sections were observed under a fluorescence microscope (Leica TCS SP8, Germany). The intensity of immunofluorescence was analyzed using Image-Pro plus 6.0 software (software Media Cybernetics, Rockville, MD, USA).

Hoechst 33258 staining

To assess the extent of apoptosis in the liver cells of T2DM mice, Hoechst 33258 staining was performed as previously described with some modifications [26]. In brief, 5-μm paraffin-embedded liver sections were stained with Hoechst 33258 solution at 10 μg·mL^{-1} for 5 min, and then the apoptotic nuclei were observed under an UV excitation fluorescence microscope (Leica TCS SP8, Germany).

Western blot

Total protein was extracted from liver tissues with RIPA buffer at ratio of 1 : 10 (*W/V*) using BCA Protein Assay Kit (Beyotime Biotechnology, Shanghai, China). Western blot was performed as previously described with modifications [27]. In this study, proteins were separated by 12% sodium dodecyl sulfate-polyacrylamide gel electrophoresis (SDS-PAGE), and then transferred to polyvinylidene fluoride membrane (PVDF). The membrane was first blocked with 5% (*W/V*) defatted milk to remove non-specific binding for 2 h, and then incubated with primary antibodies at various ratios: Akt (1 : 500), p-Akt (1 : 500), NF-*κ*B p65 (1 : 1000), p-NF-*κ*B (1 : 1000), NLRP3 (1 : 1000), ASC (1 : 1000), TNF-*α* (1 : 1000), IL-1*β* (1 : 1000), FOXO1 (1 : 1000), p-FOXO1 (1 : 1000), Caspase 1 (1 : 1000), Cleaved caspase 1 (1 : 1000), Bax (1 : 1000), Bcl-2 (1 : 1000), G6Pase (1 : 2000), and PEPCK (1 : 1000) at 4 °C overnight. *β*-Actin (1 : 1000) was used as a loading control. Then, the membrane was washed three times with TBST, and then incubated with secondary antibodies at room temperature for 2 h. Finally, the blots were detected with Emitter Coupled Logic substrates (Thermo Scientific, USA) and densitometry was performed by Image-Pro plus 6.0 software (Media Cybernetics, Rockville, MD, USA).

Molecular docking

The initial protein structure used in this study was downloaded from the protein data bank (PDB), The PDB ID for FOXO1 was 6QZS. The structure of G-Rh1 was selected from PubChem database (https://pubchem.ncbi.nlm.nih.gov/). The 3D structure of G-Rh1 was drawn using the ChemBio3D Ultra 14.0 software (Cambridge Soft Corporation, Cambridge, MA, USA). Energy minimization of small-molecule structures was performed using the MM2 energy minimization function in ChemBio3D Ultra, and utilizing PyMOL software to dehydrate the target protein receptor and remove organic matter [28]. AutoDockTools 1.5.6 software was

used to remove water molecules, perform hydrogenation, and calculate the charge of the protein. The structure was then saved in the "pdbqt" format. Finally, Vina (.exe) was run to assess molecular docking. The docking results of each core target protein and the compound with good binding ability was displayed in 3D map through PyMOL software.

Statistical analysis

Data are expressed as the means ± standard deviation (SD). Student's *t*-test was employed for comparisons between two groups. Multiple comparisons were performed using one-way ANOVA followed by Bonferroni's post hoc test. Analyses were performed using GraphPad Prism 8.0.1. (GraphPad Software, La Jolla, CA, USA). A P values of less than 0.05 or 0.01 were a statistical difference.

Results

G-Rh1 ameliorated FBG and INS Levels in T2DM mice

Insulin is a hormone which plays a crucial role in the maintenance of blood glucose levels, as well as glycogen synthesis, fat storage, and protein synthesis in the body. Deficiency or inability to respond to insulin may lead to diabetic manifestations [29]. In the current study, a significance reduction of the levels of fasting blood glucose (FBG) was observed in T2DM mice after administration with G-Rh1 for eight weeks ($P < 0.01$) (Fig. 2A). In addition, the declined insulin level in the mice of the T2DM group was relieved upon exposure to 5 and 10 mg·kg^{-1} G-Rh1 for eight weeks (Fig. 2B), demonstrating the protective effects of G-Rh1 on glucose homeostasis.

G-Rh1 relieved T2DM-induced dyslipidemia

As shown in Fig. 2, the serum levels of TC, TG, LDL-C and HDL-C in the T2DM group were significantly enhanced ($P < 0.01$) (Figs. 2C−2F). Although a slight increase in HDL-C levels showed protective effects, abnormal metabolism appeared in the liver when HDL-C was excessive [30]. In this study, HDL-C levels decreased to the baseline upon the addition of G-Rh1-H ($P < 0.05$). However, at the T2DM + G-Rh1-L group, the deteriorated indicators were not alleviated in diabetic mice.

G-Rh1 improved T2DM-induced hepatic dysfunction

AST and ALT are the primary indicators for liver functions [31]. In the present study, HFD feeding followed by STZ injection resulted in significant increased levels of ALT and AST in the T2DM group ($P < 0.01$), indicating the successful establishment of a T2DM model in mice. After administration with G-Rh1 (5 and 10 mg·kg^{-1}) for eight weeks, the elevated serum levels of ALT and AST were suppressed in diabetic mice ($P < 0.01$ or $P < 0.05$) (Figs. 2G−2H).

Furthermore, H&E staining showed that a large amount of fat vacuoles were formed in the cytoplasm of hepatocytes in the T2DM group, with weak nuclear staining, while the nuclei were squeezed to one side, or even disappeared. However, G-Rh1 administration prevented severse damage on the liver cells in a dose-dependent manner ($P < 0.01$), where the nucleus and hepatic central vein restored back to the normal at the indicated doses of G-Rh1 (Fig. 2I).

G-Rh1 regulated liver gluconeogenesis via the Akt/FOXO1 signaling pathway

According to previous reports, Akt activation inhibited FOXO1 phosphorylation, which then inhibited the expression of G6Pase and PEPCK genes, leading to the suppression of gluconeogenesis [19]. To confirm the involvement of the AKT/FOXO1 signaling pathway in gluconeogenesis, the expression of ATK, FOXO1, and G6Pase, and PEPCK was analyzed by Western blot (Figs. 3A−3C). In this study, a down-regulated FOXO1 phosphorylation by Akt was observed ($P < 0.01$). Furthermore, immunofluorescence staining demonstrated that G-Rh1 (5 and 10 mg·kg^{-1}) modulated gluconeogenesis by inhibiting the increased expression of G6Pase and PEPCK induced by T2DM in diabetic mice to various extents ($P < 0.01$) (Figs. 3D−3E).

To explore the interaction between G-Rh1 and FOXO1, an in silico molecular docking study was performed. The binding modes of G-Rh1 to FOXO1 were predicted by Autodock. As shown in Fig. 3I, G-Rh1 formed two hydrogen-bonds with FOXO1 by interacting with ASP-97 and TYR-128. The binding energy of G-Rh1 to FOXO1 was −6.9 kcal·mol^{-1}. Then, the interactions between G-Rh1 and G6Pase, and between G-Rh1 and PEPCK were investigated. The binding energy of G-Rh1 to G6Pase and PEPCK was −7.5 and −6.8 kcal·mol^{-1}, respectively.

G-Rh1 mitigated T2DM-induced inflammatory responses

Previous studies indicated that activation of NF-κB, the central inflammatory transcription factor, increased the secretion of inflammatory cytokines, such as IL-1β, IL-6 and TNF-α [32, 33]. Therefore, in the current study, we examined whether NF-κB activation was involved in the regulation of TNF-α and IL-1β expression in diabetic mice. As shown in Figs. 4A−4B, the activated NF-κB in T2DM mice stimulated the levels of TNF-α and IL-1β ($P < 0.01$), as well as the levels of NLRP3, ASC and Caspas1 ($P < 0.01$, 0.05 and 0.01 respectively), which were then reduced after G-Rh1 administration.

G-Rh1 suppressed T2DM-induced apoptosis

Hoechst 33258 staining was performed to evaluate hepatocyte apoptosis. Bax and Bcl-2 are the major regulatory genes responsible for apoptosis [34]. The two factors worked in an opposite manner, where Bcl-2 inhibits and Bax stimulates cell apoptosis. Results showed that the number of apoptotic liver cells significantly increased in the T2DM group but then decreased after G-Rh1 treatment (Figs. 5A−5B). Furthermore, G-Rh1 administration improved the over-expression and under-expression of Bax and Bcl-2 in T2DM mice, respectively, according to Western blot analysis ($p < 0.05$) (Figs. 5C−5I).

Disscussion

In type 2 diabetes mellitus (T2DM), chronic inflammation is closely associated with the development of diabetic complications, such as insulin resistance, cardiovascular diseases, and renal failure [35]. Insulin is a hormone that involves

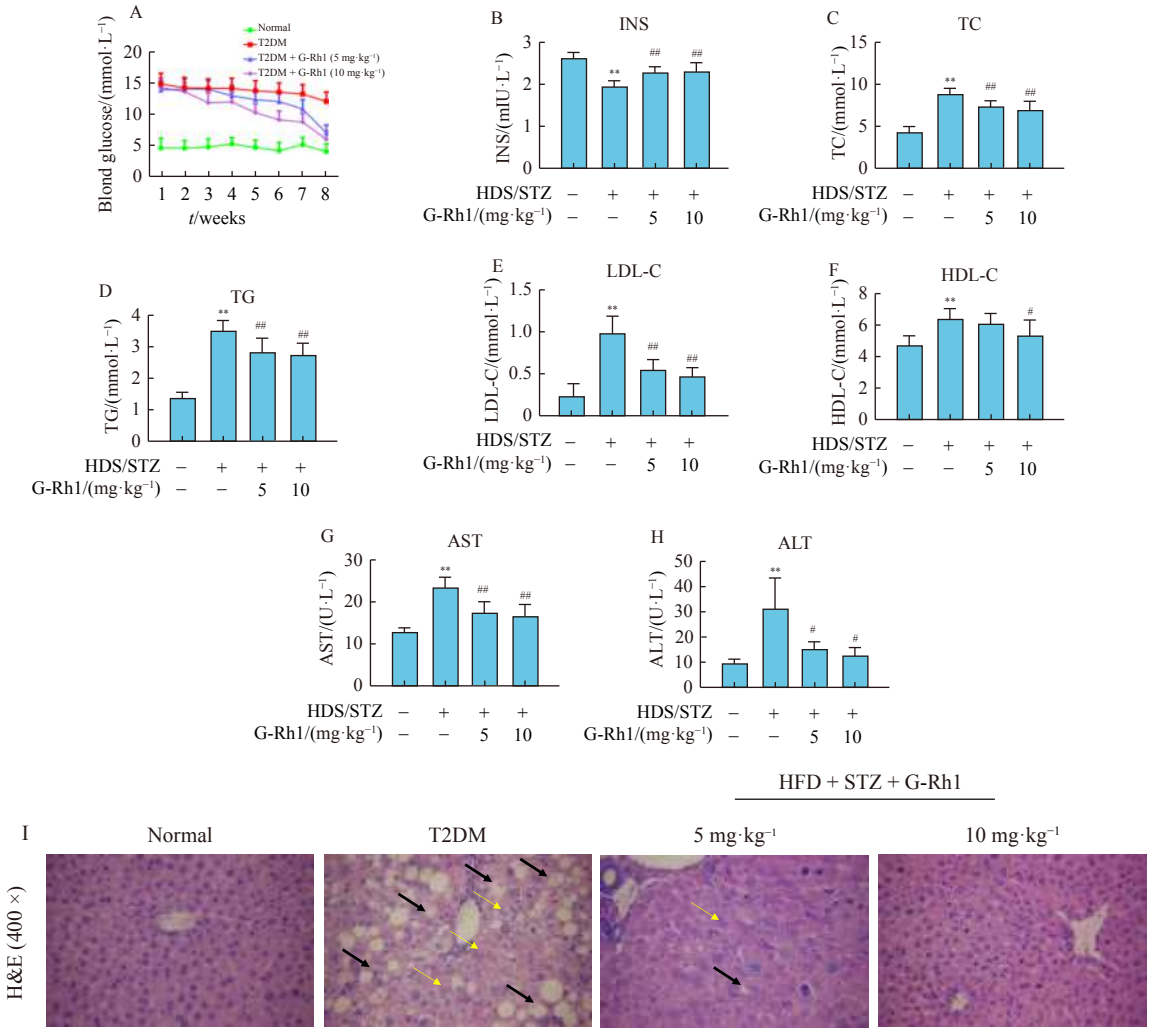

Fig. 2 G-Rh1 ameliorated blood glucose, insulin levels, dyslipidemia, and hepatic dysfunction in T2DM mice. (A) Blood glucose levels; (B) INS levels; (C) TC levels; (D) TG levels; (E) HDL-C levels; (F) LDL-C levels; (G) AST levels; (H) ALT levels; and (I) Hepatic tissues were stained by H&E dye and observed under a microscope (400 ×). Black arrows refers to the fat vacuole and yellow arrows refers to weak nuclear staining. Data are expressed as the mean ± SD (n = 10). $^{*}P < 0.05$, $^{**}P < 0.01$ *vs* the normal group; $^{\#}P < 0.05$ or $^{\#\#}P < 0.01$ *vs* the T2DM group

in the maintenance of blood glucose by converting excessive glucose in blood circulation into glycogen in tissues including the liver and muscles, keeping blood glucose at a certain level and promoting the synthesis of fats and proteins [36, 37]. However, insufficient insulin secretion and/or insulin resistance may result in glucose and lipid metabolism disorders. According to recent studies, ginsenoside Re has been found to exert anti-diabetic effect, while ginsenoside Rg1 inhibited glucagon-induced liver gluconeogenesis *via* the Akt/FOXO1 signaling pathway [19, 20].

The liver, muscle, and brain are the primary targets of insulin. The liver is the principal organ associated with glycolipid metabolism and regulation of insulin resistance in T2DM [38], and also supposed to be damaged by this disease [39]. In the current study, the levels of TC, LDL-C, TG, and HDL-C as well as the levels of ALT and AST increased in the of T2DM group, indicating liver damages in diabetic mice. However, increased serum levels of ALT and AST were reduced upon administration with G-Rh1, where the effect of 10 mg·kg^{-1} G-Rh1 was more prominent. Meanwhile, the indices of blood lipid metabolisms, such as HDL-C, LDL-C, TG, and TC were also improved.

PI3K/Akt plays a crucial role in glucose homeostasis through regulating glucose production in the liver and uptake in thr muscles and fats [40]. Prveiouis studies indicated that FOXO1, a transcription factor, was negatively regulated through phosphorylation by activating Akt (p-Akt) [41]. FOXO1 also up-regulated the expression of phosphoenolpyruvate carboxy kinase (PEPCK) and glucose-6-phosphatase (G6Pase) genes by direct binding to their regulatory sequences and through the interaction with nuclear receptors [42]. Intriguingly, molecular docking demonstrated that FOXO1 formed hydrogen bonds with ASP-97 and TYR-128 in the active pocket of G-Rh1. Consistent with previous studies [10, 11, 19], we found pronounced down-regulated expression of phosphorylated-Akt (p-Akt), as well we the increased

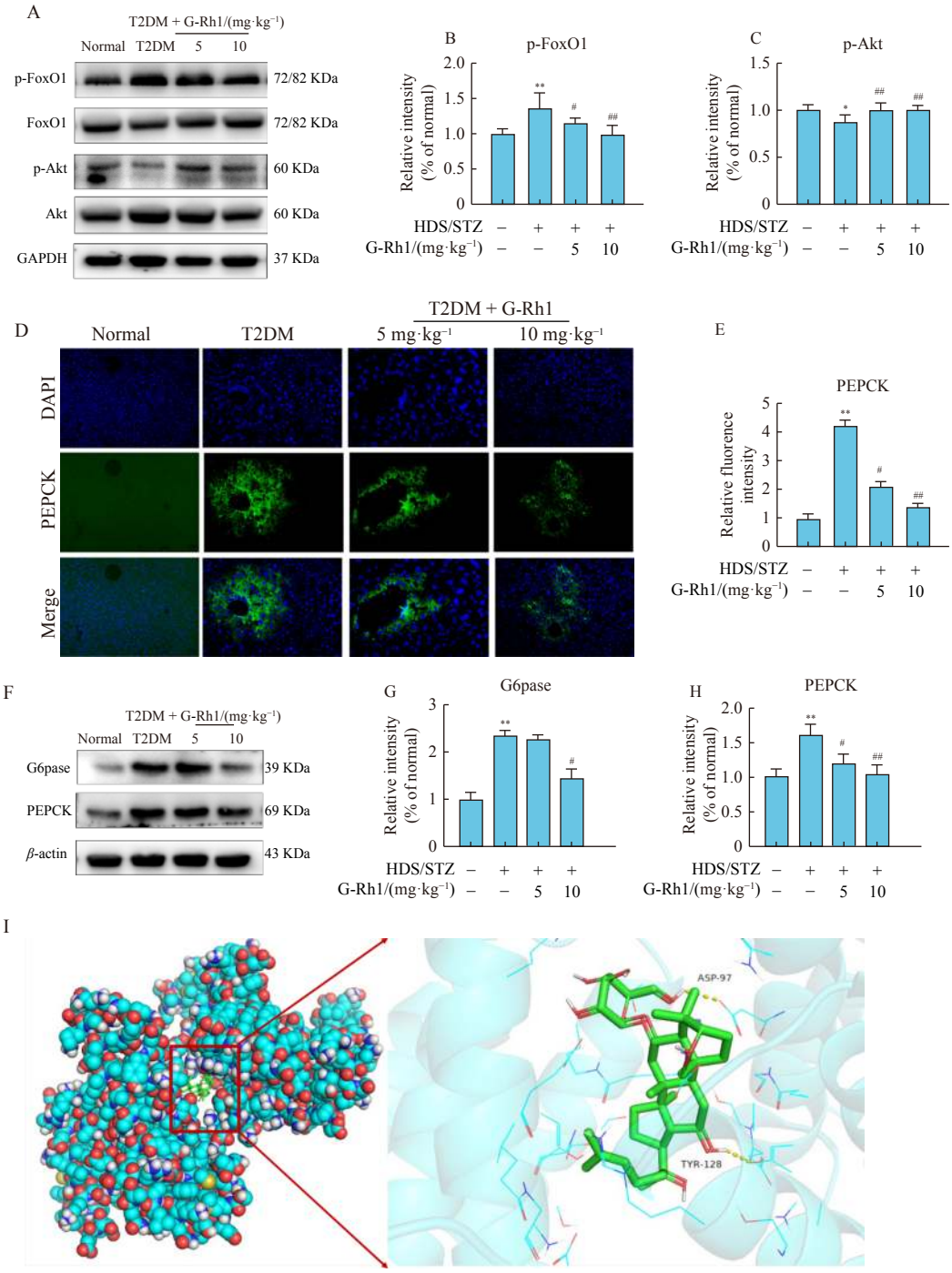

Fig. 3 G-Rh1 regulated liver gluconeogenesis *via* the Akt/FoxO1 signaling pathway. (A) Analysis of the Akt/FoxO1 signaling pathway by Western blot; (B) Expression of phosphorylated-FOXO1 (p-FOXO1) by densitometric analysis; (C) Expression of phosphorylated-Akt (p-Akt) by densitometric analysis; (D) Immunofluorescence image of the expression of PEPCK (green) in tissues from different groups; (E) Fluorescence intensities of PEPCK; (F) Expression of PEPCK and G6Pase by Western blot; (G) Expression of G6Pase by by densitometric analysis; (H) Expression of PEPCK by by densitometric analysis; and (I) Binding modes of G-Rh1 to FOXO1. Data are expressed as the mean ± SD (n = 10). $^{*}P < 0.05$, $^{**}P < 0.01$ *vs* the normal group; $^{\#}P < 0.05$, $^{\#\#}P < 0.01$ *vs* the T2DM group

expression of phosphorylated FOXO1 (p-FOXO1), PEPCK and G6Pase in T2DM mice. Western blot analysis revealed a reverse tendency of the expression of p-Akt and p-FOXO1 in the T2DM mice (Fig. 3), which were modulated after administration of G-Rh1. Furthermore, G-Rh1 efficiently reduced HFD-induced expression of gluconeogenesis enzymes, such as PEPCK and G6Pase. In the current study, G-Rh1 regulated gluconeogenesis *via* the Akt/FoxO1 signaling pathway,

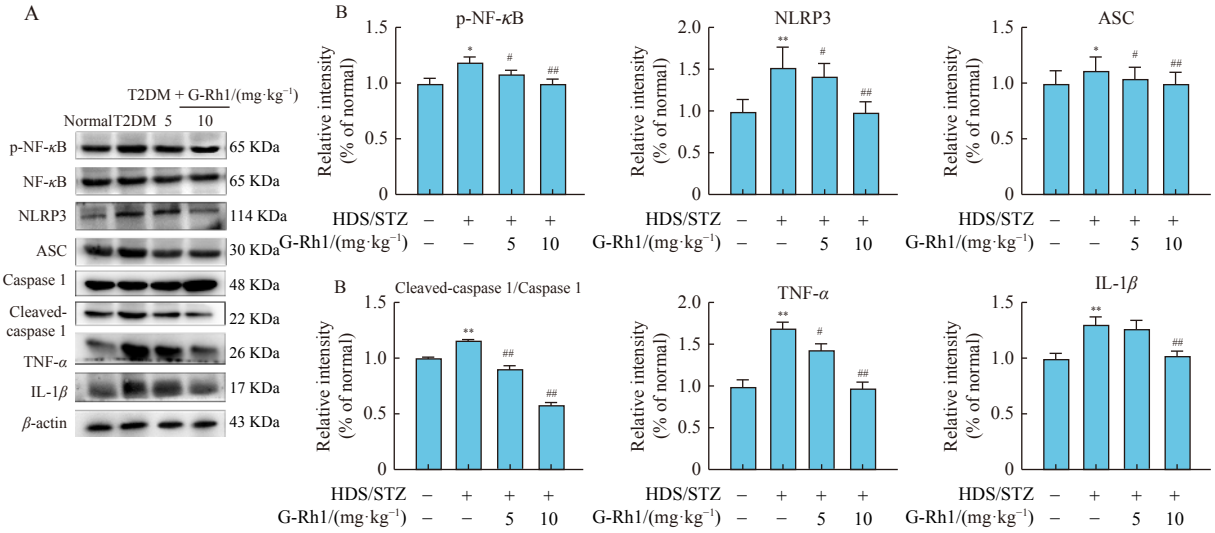

Fig. 4 G-Rh1 mitigated T2DM-induced inflammatory responses. (A) Analysis of the NF-κB signaling pathway by Western blot; (B) Expression of p-NF-κB, NLRP3, ASC, Cleaved Caspase 1/Caspase 1, TNF-α, and IL-1β by densitometric analysis. Data are expressed as the mean ± SD (n = 10). $^{*}P < 0.05$, $^{**}P < 0.01$ *vs* the normal group; $^{\#}P < 0.05$, $^{\#\#}P < 0.01$ *vs* the T2DM group

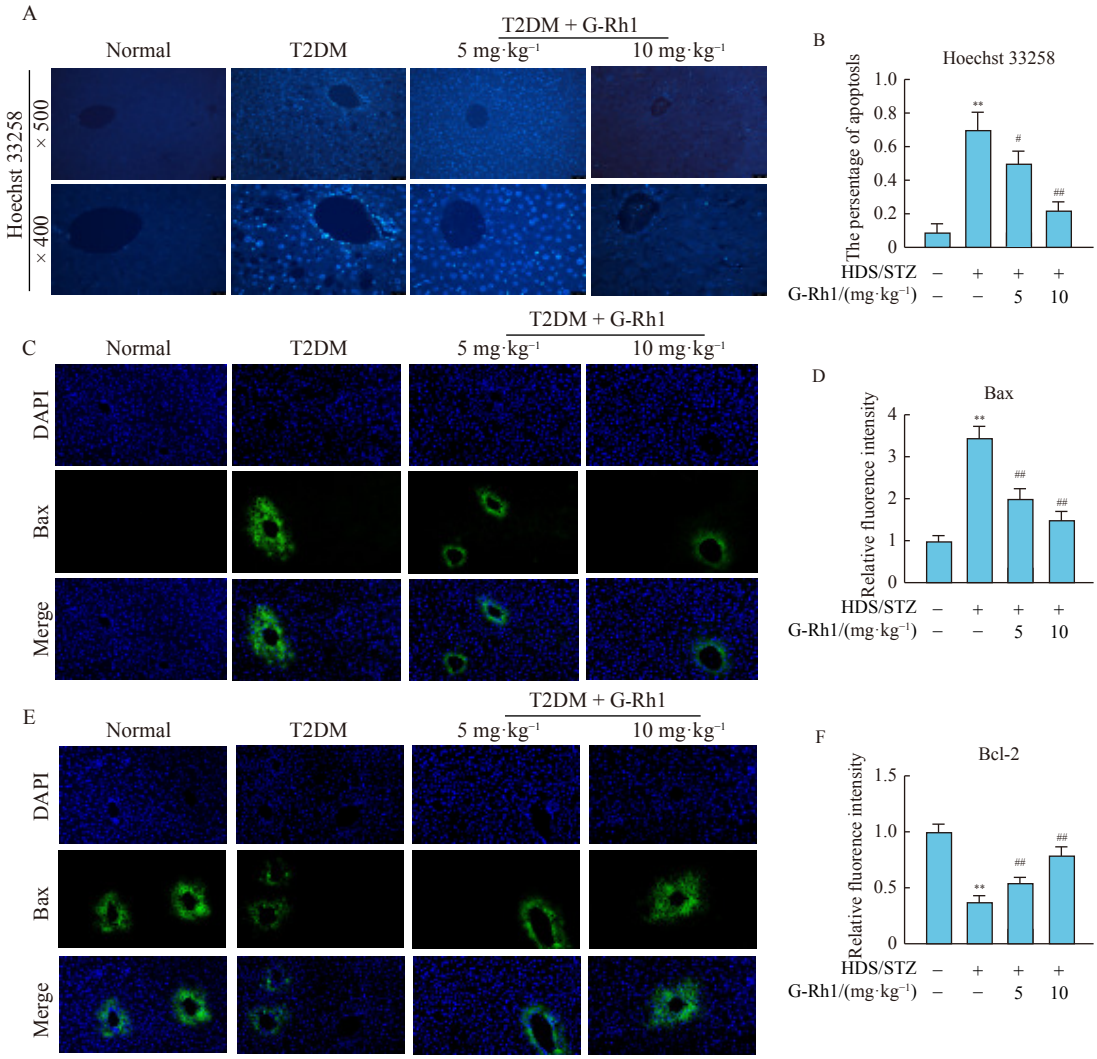

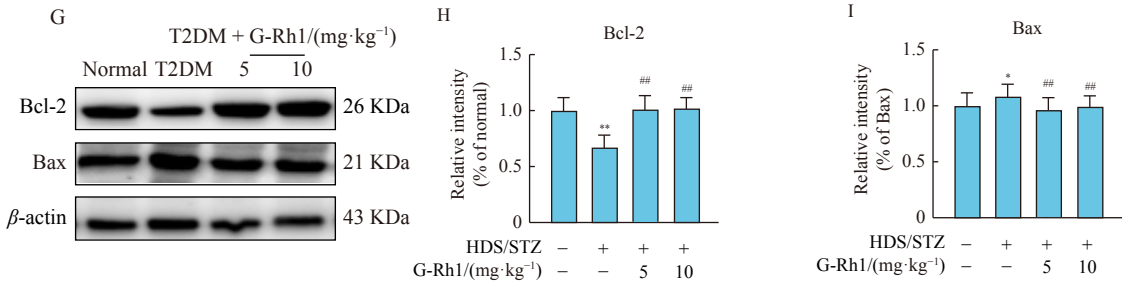

Fig. 5 G-Rh1 mitigated T2DM-induced apoptosis. (A) Hoechst 33258 staining of hepatic tissues (200 × and 400 ×); (B) Fluorescence intensity of Hoechst 33258 staining; (C) Immunofluorescence image of the expression of Bax (green) in tissues from different groups; (D) Fluorescence intensities of Bax; (E) Immunofluorescence image of the expression of Bcl-2 (green) in tissues from different groups; (F) Fluorescence intensities of Bax expression; (G) Analysis of Bax and Bcl-2 by Western blot; (H) Expression of Bcl-2 by densitometric analysis; (I) Expression of Bax by densitometric analysis. Data are expressed as the mean ± SD (n = 10). $^{*}P$ < 0.05, $^{**}P$ < 0.01 *vs* the normal group; $^{\#}P$ < 0.05, $^{\#\#}P$ < 0.01 *vs* the T2DM group

which in turn inhibited the production of hepatic glucose.

Despite a beneficial response to restore tissue homeostasis, inflammation may cause tissue injury when it is severse and maintains for a long time. Liver inflammation was likely to cause insulin resistance associated with chronic diseases such as T2DM [43, 44]. The FOXO1 and NF-κB pathways were convergent in IL-1β gene expression. Under clinical complications of obesity and diabetes, FOXO1 signaling plays an important role in coupling proinflammatory cytokines production with insulin resistance *via* NF-κB [45]. Activation of NLRP3 inflammasome promoted Caspase-1 and the subsequent release of pro-inflammatory cytokines IL-1β and IL-18 [46]. In the current study, the anti-inflammatory effects of G-Rh1 were examined through measuring the levels of NF-κB, cytokines TNF-α and IL-1β in mice treated with G-Rh1 at different doses. As expected, the increased expression of TNF-α, IL-1β and NLPR3 in T2DM mice were alleviated after administration with G-Rh1 (Fig. 4). Moreover, extensive studies have indicated that inflammatory reactions promote apoptosis [24, 47], which was also demonstrated in the current study (Fig. 5). Interestingly, a reverse trend of the expression of anti/pro-apoptotic protein Bcl-2/Bax was observed after G-Rh1 treatment, with significant up- and down-regulation of Bcl-2 and Bax, respectively. G-Rh1 showed a pronounced protective effect against liver inflammation through regulating NF-κB activity and inhibiting the expression of pro-apoptosis protein.

In conclusion, ginsenoside Rh1 shows significant preventive effect against the development of T2DM in C57BL/6 mice. Ginsenoside Rh1 is involved in the regulation of hepatic gluconeogenesis *via* the Akt/FoxO1 signal pathway. The down-regulated FOXO1 by G-Rh1 inhibits the expression of the key enzymes, PEPCK and G6Pase during gluconeogenesis, so as to regulate blood glucose levels. Furthermore, G-Rh1 can alleviate inflammatory responses and apoptosis in the liver induced by T2DM, improve liver functions by regulating the metabolism of liver glucose and lipid, and prevent the development of diabetic complications (Fig. 6). These promising findings will promote the clinical application of G-Rh1 in the treatment of T2DM.

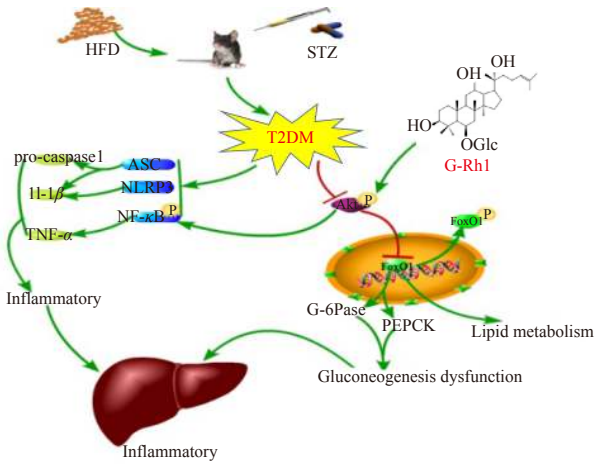

Fig. 6 The underlying mechanism of T2DM-induced inflammation and gluconeogenesis in mice

References

[1] Holman N, Young B, Gadsby R. Current prevalence of type 1 and type 2 diabetes in adults and children in the UK [J]. *Diabet Med*, 2015, **32**(9): 1119-1120.

[2] Yang J, Kang J, Guan Y. The mechanisms linking adiposopathy to type 2 diabetes [J]. *Front Med*, 2013, **7**(4): 433-444.

[3] Barazzoni R, Zanetti M, Sturnega M, *et al*. Insulin downregulates SIRT1 and AMPK activation and is associated with changes in liver fat, but not in inflammation and mitochondrial oxidative capacity, in streptozotocin-diabetic rat [J]. *Clin Nutr*, 2011, **30**(3): 384-390.

[4] Sato T, Watanabe Y, Nishimura Y, *et al*. Acute fructose intake suppresses fasting-induced hepatic gluconeogenesis through the AKT-FoxO1 pathway [J]. *Biochem Biophys Rep*, 2019, **18**: 100638.

[5] Kim DH, Kim SJ, Yu KY, *et al*. Anti-hyperglycemic effects and signaling mechanism of *Perilla frutescens* sprout extract [J]. *Nutr Res Pract*, 2018, **12**(1): 20-28.

[6] Li W, Zhang M, Gu J, *et al*. Hypoglycemic effect of protopanaxadiol-type ginsenosides and compound K on type 2 diabetes mice induced by high-fat diet combining with streptozotocin *via* suppression of hepatic gluconeogenesis [J]. *Fitoterapia*, 2012, **83**(1): 192-198.

[7] Drougard A, Duparc T, Brenachot X, *et al*. Hypothalamic apelin/reactive oxygen species signaling controls hepatic glucose metabolism in the onset of diabetes [J]. *Antioxid Redox Signal*, 2014, **20**(4): 557-573.

[8] Galbo T, Perry RJ, Nishimura E, *et al*. PP2A inhibition results in hepatic insulin resistance despite Akt2 activation [J]. *Aging (Albany NY)*, 2013, **5**(10): 770-781.

[9] Wu Z, Qiu M, Mi Z, *et al*. WT1-interacting protein inhibits cell proliferation and tumorigenicity in non-small-cell lung cancer *via* the AKT/FOXO1 axis [J]. *Mol Oncol*, 2019, **13**(5): 1059-1074.

[10] Wu Z, Jiao P, Huang X, *et al*. MAPK phosphatase-3 promotes hepatic gluconeogenesis through dephosphorylation of forkhead box O1 in mice [J]. *J Clin Invest*, 2010, **120**(11): 3901-3911.

[11] Zhang Y, Aguilar OA, Storey KB. Transcriptional activation of muscle atrophy promotes cardiac muscle remodeling during mammalian hibernation [J]. *Peer J*, 2016, **4**: e2317.

[12] Taghian T, Metelev VG, Zhang S, *et al*. Imaging NF-kappaB activity in a murine model of early stage diabetes [J]. *FASEB J*, 2020, **34**(1): 1198-1210.

[13] Song W, Wei L, Du Y, *et al*. Protective effect of ginsenoside metabolite compound K against diabetic nephropathy by inhibiting NLRP3 inflammasome activation and NF-kappaB/p38 signaling pathway in high-fat diet/streptozotocin-induced diabetic mice [J]. *Int Immunopharmacol*, 2018, **63**: 227-238.

[14] Che H, Wang Y, Li H, *et al*. Melatonin alleviates cardiac fibrosis *via* inhibiting lncRNA MALAT1/miR-141-mediated NLRP3 inflammasome and TGF-beta1/Smads signaling in diabetic cardiomyopathy [J]. *FASEB J*, 2020, **34**(4): 5282-5298.

[15] He Y, Hara H, Nunez G. Mechanism and regulation of NLRP3 inflammasome activation [J]. *Trends Biochem Sci*, 2016, **41**(12): 1012-1021.

[16] Ohtake F, Takeyama K, Matsumoto T, *et al*. Modulation of oestrogen receptor signalling by association with the activated dioxin receptor [J]. *Nature*, 2003, **423**(6939): 545-550.

[17] Yang JY, Kang MY, Nam SH, *et al*. Antidiabetic effects of rice hull smoke extract in alloxan-induced diabetic mice [J]. *J Agric Food Chem*, 2012, **60**(1): 87-94.

[18] Alolga RN, Nuer-Allornuvor GF, Kuugbee ED, *et al*. Ginsenoside Rg1 and the control of inflammation implications for the therapy of type 2 diabetes: a review of scientific findings and call for further research [J]. *Pharmacol Res*, 2020, **152**: 104630.

[19] Liu Q, Zhang FG, Zhang WS, *et al*. Ginsenoside Rg1 inhibits glucagon-induced hepatic gluconeogenesis through Akt-FoxO1 interaction [J]. *Theranostics*, 2017, **7**(16): 4001-4012.

[20] Cho WC, Chung WS, Lee SK, *et al*. Ginsenoside Re of *Panax ginseng* possesses significant antioxidant and antihyperlipidemic efficacies in streptozotocin-induced diabetic rats [J]. *Eur J Pharmacol*, 2006, **550**(1-3): 173-179.

[21] Jia W, Gao W, Tang L. Antidiabetic herbal drugs officially approved in China [J]. *Phytother Res*, 2003, **17**(10): 1127-1134.

[22] Yu S, Zhou X, Li F, *et al*. Microbial transformation of ginsenoside Rb1, Re and Rg1 and its contribution to the improved anti-inflammatory activity of ginseng [J]. *Sci Rep*, 2017, **7**(1): 138.

[23] Quan LH, Min JW, Sathiyamoorthy S, *et al*. Biotransformation of ginsenosides Re and Rg1 into ginsenosides Rg2 and Rh1 by recombinant beta-glucosidase [J]. *Biotechnol Lett*, 2012, **34**(5): 913-917.

[24] Li Y, Hou JG, Liu Z, *et al*. Alleviative effects of 20(*R*)-Rg3 on HFD/STZ-induced diabetic nephropathy *via* MAPK/NF-kappaB signaling pathways in C57BL/6 mice [J]. *J Ethnopharmacol*, 2021, **267**: 113500.

[25] Liu W, Wang Z, Hou JG, *et al*. The liver protection effects of maltol, a flavoring agent, on carbon tetrachloride-induced acute liver injury in mice *via* inhibiting apoptosis and inflammatory response [J]. *Molecules*, 2018, **23**(9): 2120.

[26] Liu W, Wang Z, Leng J, *et al*. 20(*R*)-ginsenoside Rg3, a product of high-efficiency thermal deglycosylation of ginsenoside Rd, exerts protective effects against scrotal heat-induced spermatogenic damage in mice [J]. *Biocell*, 2020, **44**(4): 655-669.

[27] Leng J, Wang Z, Fu CL, *et al*. NF-kappaB and AMPK/PI3K/Akt signaling pathways are involved in the protective effects of *Platycodon grandiflorum* saponins against acetaminophen-induced acute hepatotoxicity in mice [J]. *Phytother Res*, 2018, **32**(11): 2235-2246.

[28] Chen X, Song J, Yuan D, *et al*. Incaspitolide A extracted from *Carpesium cernuum* induces apoptosis *in vitro via* the PI3K/AKT pathway in benign prostatic hyperplasia [J]. *Biosci Rep*, 2021. **41**(6): BSR20210477.

[29] Ma ZN, Li YZ, Li W, *et al*. Nephroprotective effects of saponins from leaves of *Panax quinquefolius* against cisplatin-induced acute kidney injury [J]. *Int J Mol Sci*, 2017. **18**(7): 1407.

[30] Barter PJ, Nicholls S, Rye KA, *et al*. Antiinflammatory properties of HDL [J]. *Circ Res*, 2004, **95**(8): 764-772.

[31] Ni J, Zhao Y, Su J, *et al*. Toddalolactone protects lipopolysaccharide-induced sepsis and attenuates lipopolysaccharide-induced inflammatory response by modulating HMGB1-NF-kappaB translocation [J]. *Front Pharmacol*, 2020, **11**: 109.

[32] Jin Y, Liu L, Chen B, *et al*. Involvement of the PI3K/Akt/NF-kappaB signaling pathway in the attenuation of severe acute pancreatitis-associated acute lung injury by *Sedum sarmentosum* Bunge extract [J]. *Biomed Res Int*, 2017, **2017**: 9698410.

[33] Bunting K, Rao S, Hardy K, *et al*. Genome-wide analysis of gene expression in T cells to identify targets of the NF-kappa B transcription factor c-Rel [J]. *J Immunol*, 2007, **178**(11): 7097-7109.

[34] Youle RJ, Strasser A. The BCL-2 protein family: opposing activities that mediate cell death [J]. *Nat Rev Mol Cell Biol*, 2008, **9**(1): 47-59.

[35] Downs CA, Faulkner MS. Toxic stress, inflammation and symptomatology of chronic complications in diabetes [J]. *World J Diabetes*, 2015, **6**(4): 554-565.

[36] Batista TM, Dagdeviren S, Carroll SH, *et al*. Arrestin domain-containing 3 (Arrdc3) modulates insulin action and glucose metabolism in liver [J]. *Proc Natl Acad Sci U S A*, 2020, **117**(12): 6733-6740.

[37] Coussa A, Bassil M, Gougeon R, *et al*. Glucose and protein metabolic responses to an energy, but not protein, restricted diet in type 2 diabetes [J]. *Diabetes Obes Metab*, 2020, **22**(8): 1278-1285.

[38] Meng XH, Chen B, Zhang JP. Intracellular insulin and impaired autophagy in a zebrafish model and a cell model of type 2 diabetes [J]. *Int J Biol Sci*, 2017, **13**(8): 985-995.

[39] Cheng FR, Cui HX, Fang JL, *et al*. Ameliorative effect and mechanism of the purified anthraquinone-glycoside preparation from *Rheum palmatum* L. on Type 2 diabetes mellitus [J].

Molecules, 2019, **24**(8): 1454.

[40] Huang X, Liu G, Guo J, *et al*. The PI3K/AKT pathway in obesity and type 2 diabetes [J]. *Int J Biol Sci*, 2018, **14**(11): 1483-1496.

[41] Wang C, Hamacher A, Petzsch P, *et al*. Combination of decitabine and entinostat synergistically inhibits urothelial bladder cancer cells *via* activation of FoxO1 [J]. *Cancers (Basel)*, 2020, **12**(2): 337.

[42] Sekine K, Chen YR, Kojima N, *et al*. Foxo1 links insulin signaling to C/EBPalpha and regulates gluconeogenesis during liver development [J]. *EMBO J*, 2007, **26**(15): 3607-3615.

[43] Jovanovic SS, Martinovic V, Bogojevic D, *et al*. Modulation of diabetes-related liver injury by the HMGB1/TLR4 inflammatory pathway [J]. *J Physiol Biochem*, 2018, **74**(2): 345-358.

[44] Gao Y, Li J, Chu S, *et al*. Ginsenoside Rg1 protects mice against streptozotocin-induced type 1 diabetic by modulating the NLRP3 and Keap1/Nrf2/HO-1 pathways [J]. *Eur J Pharmacol*, 2020, **866**: 172801.

[45] Su D, Coudriet GM, Hyun KD, *et al*. FoxO1 links insulin resistance to proinflammatory cytokine IL-1beta production in macrophages [J]. *Diabetes*, 2009, **58**(11): 2624-2633.

[46] Svadlakova T, Hubatka F, Turanek KP, *et al*. Proinflammatory effect of carbon-based nanomaterials: *in vitro* study on stimulation of inflammasome NLRP3 *via* destabilisation of lysosomes [J]. *Nanomaterials (Basel)*, 2020. **10**(3): 418.

[47] Xue R, Yang J, Jia L, *et al*. Mitofusin2, as a protective target in the liver, controls the balance of apoptosis and autophagy in acute-on-chronic liver failure [J]. *Front Pharmacol*, 2019, **10**: 601.

Cite this article as: SU Wen-Ya, FAN Mei-Ling, LI Ying, HU Jun-Nan, CAI En-Bo, ZHU Hong-Yan, SONG Ming-Jie, LI Wei. Protective Effects of G-Rh1 on T2DM-induced Liver Injury [J]. *Chin J Nat Med*, 2022, **20**(9): 669-678.